NEURO-OPHTHALMOLOGY
2024, VOL. 48, NO. 6, 417–428
https://doi.org/10.1080/01658107.2024.2341769

Taylor & Francis
Taylor & Francis Group

ORIGINAL ARTICLE

Ellipsoid Zone Reflectivity: Exploring its Potential as a Novel Non-Invasive Biomarker for Assessing Mitochondrial Function

I. Kleerekooper[a,b,c], D.V. Verschueren, S.A. Trip[b,d], G.T. Plant[e], and A. Petzold[a,b,c,f]

[a]Department of Brain Repair and Rehabilitation, Moorfields Eye Hospital NHS Foundation Trust, UCL, London, UK; [b]Queen Square MS Centre, Department of Neuroinflammation, UCL Institute of Neurology, Faculty of Brain Sciences, University College London, London, UK; [c]Department of Neurology, Amsterdam University Medical Center, Amsterdam, Netherlands; [d]Biomedical Research Centre, National Institute for Health Research (NIHR), University College London Hospitals (UCLH), London, UK; [e]Department of Brain Repair and Rehabilitation, University College London, London, UK; [f]Dutch Expertise Centre for Neuro-Ophthalmology, MS Centre, Departments of Neurology & Ophthalmology, Amsterdam UMC, Amsterdam, The Netherlands

ABSTRACT

The ellipsoid zone (EZ) on macular optical coherence tomography (OCT) scans exhibits high intensity due to a high density of light-scattering mitochondria, making its reflectivity a potential marker for mitochondrial function. Here, we developed a reliable analysis tool for extracting relative EZ reflectivity and explore its potential as a biomarker in various diseases. We analysed OCT scans of patients with optic neuritis (ON), primary progressive optic neuropathy (PPON), chronic progressive external ophthalmoplegia (CPEO), dominant optic atrophy (DOA), and healthy controls. EZ reflectivity (normalised to the retina pigment epithelium (RPE) and outer nuclear layer (ONL)) was evaluated. Reliability was assessed using intraclass correlation coefficients (ICC), and group differences were analysed through multivariable linear regression, adjusting for relevant confounders. In total, 12 controls, 23 ON patients, 7 CPEO patients, 13 DOA patients, and 13 PPON patients were included. EZ/RPE20% and EZ/ONL ratios demonstrated good test–retest reliability with ICCs of 0.76 ($p < .001$) and 0.63 ($p = .013$), respectively. Multivariable regression analysis revealed that median EZ/RPE20% and EZ/ONL ratios were lower in CPEO ($r = -0.12$, $p = .036$, and $r = -0.59$, $p = .011$), DOA ($r = -0.16$, $p = .049$, and $r = -0.55$, $p = .082$), PPON ($r = -0.17$, $p = .014$, and $r = -0.57$, $p = .037$), and ON ($r = -0.11$, $p = .013$, and $r = -0.42$, $p = .006$) compared to controls, respectively. These data show that EZ reflectivity can be reliably determined from OCT scans and appears to be reduced in neuroinflammatory and mitochondrial disorders. Further validation in larger prospective cohorts is warranted, but our findings suggest that EZ reflectivity might serve as a non-invasive in-vivo biomarker for mitochondrial health.

ARTICLE HISTORY
Received 10 October 2023
Revised 9 March 2024
Accepted 8 April 2024

KEYWORDS
Mitochondria; OCT; multiple sclerosis; biomarker; retinal imaging; neuroinflammatory disease

Introduction

Mitochondrial dysfunction has been implicated in the pathophysiology of various systemic diseases, including multiple sclerosis (MS). However, research in this field faces challenges due to the lack of available non-invasive in-vivo testing.[1] Optical coherence tomography (OCT) is a non-invasive retinal imaging technique that can visualise retinal tissue structure and delineate boundaries between retinal layers based on refractive index differences. While OCT allows for the calculation of individual retinal thicknesses, the analysis of a layer's reflectivity index itself remains a novel and under-explored technique. Nevertheless, this approach holds exciting potential for studying cellular function in vivo.

Recent research combining histopathological analysis and OCT images of retinal tissue from human donor eyes revealed that the ellipsoid zone (EZ) may exhibit high reflectivity due to local mitochondrial accumulation.[2,3] This mitochondrial contribution to EZ reflectivity aligns with the anatomical structure of the EZ, with the outer portion of the inner segments of photoreceptors primarily consisting of accumulated mitochondria. Photoreceptors, particularly cones, have a high mitochondrial density.[4] As the distribution of cones changes rapidly moving away from the fovea, retinal morphology affects light scattering patterns significantly.[5] Mitochondria and lysosomes are identified as the organelles that scatter the most

CONTACT I. Kleerekooper i.kleerekooper@amsterdamumc.nl Afdeling Neurologie, de Boelelaan 1117, Amsterdam 1081 HV, The Netherlands
Supplemental data for this article can be accessed online at https://doi.org/10.1080/01658107.2024.2341769.

light in the cell, and their optical properties, particularly scattering coefficients, are associated with their structural integrity and functional status. [6–10] However, there exists controversy on the anatomical origin of the hyperreflective band, with other research, particularly within the adaptive optics community, indicating it represents the junction between the inner and outer segments of the photoreceptors.[11,12]

Regardless of its anatomical origin, preliminary data suggest associations of EZ reflectivity on OCT with age, glaucoma, and age-related macular degeneration (AMD).[11,13–17] Currently, its potential implications for MS and mitochondrial disorders remain unexplored. Given the involvement of mitochondrial failure in MS pathophysiology,[18,19] investigating EZ reflectivity in individuals affected by MS, as well as in two mitochondrial disorders – dominant optic atrophy (DOA) and chronic progressive external ophthalmoplegia (CPEO) – could offer valuable insights into metabolic function.

The primary aim of this study is to develop an automated analysis tool that extracts reflectivity data from macular OCT scans and to explore the reproducibility of the resulting measure of relative EZ reflectivity. The secondary aim is to investigate if relative EZ reflectivity could serve as an in vivo metric of mitochondrial health by exploring its potential alteration in MS, optic neuritis (ON), CPEO, and DOA.

By elucidating the relationship between EZ reflectivity and mitochondrial function, this study seeks to contribute to a better understanding of mitochondrial involvement in MS and mitochondrial disorders, potentially paving the way for non-invasive monitoring of mitochondrial health in clinical settings.

Methods

Participants

A prospective recruitment was conducted at Moorfields Eye Hospital, enrolling patients aged 18–55 years presenting with symptomatically unilateral optic neuritis (ON) without prior episodes in the affected eye. Diagnosis was confirmed by a neuro-ophthalmologist (AP) following an international consensus investigation protocol.[20] Patients presenting within 14 days of onset of visual loss and/or pain on eye movement, whichever was earlier, were included in the study. Based on specific criteria, patients were categorised into three groups: MOG-associated ON (MOGON) for those seropositive for MOG antibodies, MS-associated ON (MSON) based on the 2017 MS criteria, and single episode isolated ON (SION).[20]

Additionally, a retrospective chart review at Moorfields Eye Hospital and the Amsterdam University Medical Centre identified patients with primary progressive optic neuropathy (PPON), representing early and pronounced optic nerve involvement in MS.[20] Patients diagnosed with chronic progressive external ophthalmoplegia (CPEO) and dominant optic atrophy (DOA) were also identified through chart review at Moorfields Eye Hospital. For these retrospectively identified subjects, relevant data such as age, sex, best corrected visual acuity (BCVA), and additional medical history were recorded.

Healthy control participants were recruited from Moorfields Eye Hospital staff. Control subjects met specific criteria, including: BCVA of ≥6/6 in both eyes; absence of pre-existing eye disease; no medication usage; normal fundus appearance; and basic structural OCT measurements (peripapillary retinal nerve fibre layer (pRNFL) and macular ganglion cell-inner plexiform layer (mGCIPL)) within normal limits.

Approval for the study was obtained from the Ethics committee (study number 64,861) and hospital R&D (FRAC0001 & CaRS_23). Informed consent in writing was obtained from all prospectively enrolled subjects, in accordance with the Declaration of Helsinki. The analysis of retrospective data was exempted from review by NHS ethical committee in the UK. The Amsterdam Institutional Review Board issued a waiver stating that the requirements of the Medical Research Involving Human Subjects Act did not apply for the use of the clinical and imaging data for this study.

Informed written consent was obtained from all prospectively enrolled subjects involved in this study. Consent was waived for retrospectively identified subjects.

OCT protocol

For healthy controls and ON patients the OCT measurements were performed prospectively with Spectralis SD-OCT (Heidelberg Engineering, Inc, Heidelberg, Germany) with the eye tracking function enabled, on acquisition software version 6.7.13.0. Macular volume scan (1024 A-scans, 37 B-scans volume = 15×15°, automatic real-time function [ART] = 25) centred around the fovea with high-resolution setting enabled were performed, with subsequent scans performed on follow-up mode. Scans were consistently performed for the left eye first.

Clinically performed OCT scans were retrospectively identified for patients with PPON, CPEO, and DOA. Macular volume scans centred on the fovea that passed OSCAR-IB quality control criteria were included and analysed in this study.[21] Scan quality was approximated through the signal-to-noise ratio and was set at a minimum of 20 dB for inclusion.

A subset of subjects completed a repeated-measures protocol of performing two scans separated by a 1 h interval to explore test–retest reliability. This occurred in a controlled research setting.

OCT layer segmentation

Macular OCT scans were segmented for quantitative thickness data with OCTExplorer (Version 3.8.0 (x64)) from IOWA Reference Algorithms. This algorithm segmented the retinal nerve fibre layer (RNFL), ganglion cell layer (GCL), inner plexiform layer (IPL), inner nuclear layer (INL), outer plexiform layer (OPL), outer nuclear layer (ONL), EZ, outer segments (OS), outer segment of the photoreceptor/RPE complex including subretinal potential space (OPR) and RPE. The mGCIPL was created by combining the GCL and IPL. The inner retinal layers (IRL) were created by combining all layers that were located above the EZ, being the RNFL, GCL, IPL, INL, OPL, and ONL. Thicknesses were calculated in a 1, 3, and 6 mm ETDRS grid. Layer segmentation was visually inspected and manually corrected where required.

Reflectivity analysis

To prepare for reflectivity analysis, macular OCT scans (.vol) were exported from Heyex in 8-bit colour depth (256 greyscale values). Images were not changed in brightness or contrast. Subsequently, images were imported in OCTExplorer (Version 3.8.0 (x64)) from IOWA Reference to be segmented. OCTExplorer instead of Heyex software was used for segmentation, as Heyex does not segment the EZ separately. Segmentation was inspected for errors and manually corrected where required. The foveal B-scan was identified and this segmented scan showing coloured layer delineation (Figure 1) was exported from OCTExplorer. Subsequently, OCT reflectivity data were extracted from this segmented image using a custom-built script in Python (Python Software Foundation; http://www.python.org/). This script extracted the grey value (0=black to 255=white) of each pixel within the segmented layers and calculated the median grey value of each layer. For the RPE the median of the 20%, 10% and 5% highest reflective pixels were calculated as well. Relative EZ reflectivity was calculated by normalising to other retinal layers separately through taking the ratio (EZ reflectivity/other layer reflectivity). Choice of reference layer is complex as each layer has advantages and disadvantages. Two metrics for relative EZ reflectivity were obtained by normalising the EZ reflectivity to both the ONL and RPE reflectivity (with the median reflectivity of the entire layer and of the 20% highest intense pixels used, respectively). Analysing these two metrics in conjunction provides robustness and ensures that identified changes are the result of changes in EZ reflectivity alone.

Data exploration

Continuous data were explored using histograms and dot-plots, while categorical data was explored using cross-tabulations. Given the low sample size non-normal distributions were assumed without formal testing; summary statistics for continuous variables were given with medians and ranges, and non-parametric tests were used. EZ reflectivity was

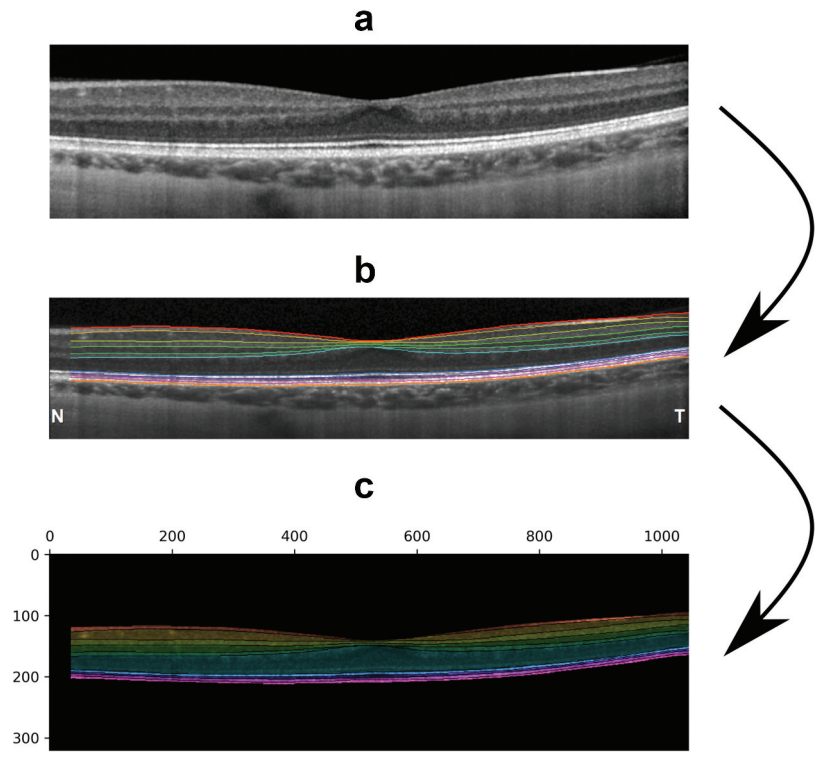

Figure 1. Flowchart showing the reflectivity data analysis process. (a) High-quality OCT scans centred on the fovea were identified using Heyex. (b) Layer segmentation was performed in OCTExplorer, and the foveal image with colour-delineated layer segmentation was exported for Python analysis. (c) Our python script identified the layer boundaries and calculated the median pixel intensity of each layer. This image was created as a check to be visually inspected for errors.

analysed for one eye per subject, to account for inter-eye correlations, except when inter-eye differences or correlations were analysed.[22] For analyses including all subjects, either the left eye or the clinically unaffected eye for ON patients was included, except when explicitly stated otherwise.

Reliability of EZ reflectivity measurement

Performance of the relative EZ reflectivity metrics with regard to reproducibility and reliability was analysed from the repeated-measures. Three measures of reliability were calculated with intraclass correlation coefficients (ICC), a measure that reflects not only the correlation but also the degree of agreement between measurements.[23] Interocular correlation was analysed by comparing the foveal B-scans of the right and left eye. Finally, to investigate intra-ocular reproducibility the correlation of the EZ reflectivity ratio between the foveal and the peripheral B-scans were analysed. For visualisation purposes, dot-plots with Spearman's correlation coefficients and associated p-value from linear regression for the association were created for these three metrics. Bland-Altman plots were used to visualise test–retest reliability. To explore if macular location influences the EZ reflectivity ratio, EZ reflectivity was compared between B-scans centred foveally and peripherally within the same eye using Wilcoxon signed-rank tests. For the peripheral scan, the middle B-scan within the field superior to the fovea within the EDTRS grid was chosen. Due to differences in scan protocols, this location may have differed slightly between subjects. This is important as photoreceptor topography, particularly photoreceptor distribution, changes dramatically away from the fovea.[5] The EZ is known to become less distinct with eccentricity. Mitochondrial density in the EZ is lower for rods than for cones, and the proportion of rods increases moving away from the fovea.[11]

Reproducibility was calculated for relative EZ reflectivity as normalised to the RPE and the ONL as potential reference layers. The RPE was chosen due to its similar intensity profile to the EZ and the ONL due to its large size.

The strength of correlation was considered as good-to-excellent (ICC/ρ > 0.75), moderate-to-good (ICC/ρ = 0.5–0.75), fair (ICC/ρ = 0.2–0.49), or not correlated (ICC/ρ < 0.25).[24]

EZ reflectivity in disease

Differences in relative EZ reflectivity were compared between the healthy controls and patients with chronic disease (PPON, CPEO, and DOA) with the Kruskal–Wallis test. If statistically significant, post-hoc evaluation was performed with the Dunn-test with p-values adjusted for multiple comparisons with the Benjamin–Hochberg method. Differences in relative EZ reflectivity (normalised to the ONL and the RPE) were compared between the healthy controls and both the affected and the fellow eyes of acute ON patients with the Wilcoxon rank-sum test.

To account for potential confounding by age, sex, retinal thickness, and scan quality, multivariable linear regression models were built. Three separate metrics of retinal thickness were considered, being GCIPL, EZ and IRL thickness. Associations of potential confounders (age, retinal thickness, and scan quality) with the outcome (EZ reflectivity) were explored through univariable linear regression. Differences in EZ reflectivity across sex were investigated with the Wilcoxon rank-sum test.

Subsequently, a multivariable linear regression model was built that included a variable for pathology with additional covariates for identified potential confounders. Finally, two multivariable linear regression analyses that were adjusted for relevant confounders were built to compare EZ reflectivity between controls and affected as well as fellow eyes of acute ON patients.

Group comparisons were performed for EZ reflectivity normalised to the RPE as well as to the ONL. This was done to check for consistency across these two metrics, to affirm that observed group differences are the result of changes to the EZ and not to either reference layer.

Statistical analysis

Significance thresholds were set to $p < .05$. Statistical analysis was performed with R and Rstudio (RStudio Team 2021, http://www.rstudio.com/).

Results

Participants

The study included a total of 23 patients with acute clinically unilateral ON, seven patients with chronic progressive external ophthalmoplegia (CPEO), 13 patients with dominant optic atrophy (DOA), 13 patients with primary progressive optic neuropathy (PPON), and 12 healthy control subjects. Baseline characteristics of the participants are presented in Table 1. Among the acute ON patients, the median best corrected visual acuity (BCVA) was 6/5 (range: 6/4–6/5) in the fellow eye and 6/9 (range: 6/6–6/60) in the affected eye. Notably, two of the acute ON patients were diagnosed with MSON and one with MOGON.

Reliability EZ reflectivity metric

The reliability of the created EZ reflectivity metrics was analysed by calculating the ICC between the two repeated scans, between the right and left eye (inter-ocular correlation) and between the foveal and the peripheral B-scan on the same eye (intra-ocular correlation). For this analysis, 12 subjects (9 healthy controls, 3 acute ON patients) had repeated-measures data available. When using the RPE as the reference layer, the best repeatability performance

Table 1. Baseline characteristics of the cohort. GCIPL = ganglion cell and inner plexiform layer. IRL = inner retinal layers. 1 = Fisher's exact test. 2 = Kruskal–Wallis test.

	Healthy controls	Acute ON patients	CPEO	DOA	PPON	*p*-value
N	12	23	7	13	13	
Sex, F (%)	6 (50%)	18 (78%)	3 (43%)	8 (61.5%)	2 (15%)	**0.018**[1]
Age years, median (range)	28.1 (27–46)	28.4 (25–28)	68.3 (18–80)	27.6 (7–70)	37.9 (22–60)	**0.044**[2]
GCIPL µm, median (range)	84.5 (72.7–95.0)	74.7 (52.6–92.1)	76.9 (52.5–81.9)	41.0 (32.3–57.6)	46.8 (32.8–64.7)	**<0.001**[2]
IRL µm, median (range)	311 (288–331)	293 (263–332)	283 (256–304)	234 (217–257)	250 (217–298)	**<0.001**[2]
ORL µm, median (range	31 (27–34)	32 (26–36)	29 (25–31)	30 (26–32)	31 (28–31)	**0.761**
EZ µm, median (range)	14.7 (13.6–16.3)	14.2 (12.9–15.9)	14.3 (12.8–15.3)	14.7 (13.5–15.4)	14.6 (13.3–15.4)	**0.367**
Scan quality dB, median (range)	38 (27–43)	35 (20–43)	27 (21–33)	28 (25–31)	27 (20–38)	**0.007**[2]

Table 2. Performance on reliability metrics (intra-class coefficients) for the EZ/RPE and EZ/ONL ratios. Test–retest ICC: intra-session repeatability between repeat scans. Interocular ICC: inter-eye agreement between right and left eye. Intra-ocular ICC: intra-eye agreement between foveal and peripheral scan within one eye. ρ = Spearman's correlation coefficient. EZ/RPE20% and EZ/ONL ratios demonstrated the highest overall reliability.

Ratio	Test-retest ICC	*p*-value	Inter-ocular ICC	*p*-value	Intra-ocular ICC	*p*-value
EZ/RPE	0.75	**<.001**	0.73	**.003**	0.16	.294
EZ/RPE20%	0.76	**<.001**	0.73	**.003**	0.35	.219
EZ/ONL	0.63	**.013**	0.65	**.009**	0.37	.102

was achieved when using the median of the 20% most intense pixels (EZ/RPE20% ratio). Test-retest and interocular ICCs were slightly better for the EZ/RPE20% ratio at 0.76 ($p < .001$) and 0.73 ($p = .003$), respectively, compared with the EZ/ONL ratio at 0.63 ($p = .013$) and 0.65 ($p = .009$). These results correspond to a 'good-to-excellent' and a 'moderate-to-good' reliability performance for the EZ/RPE20% and EZ/ONL ratios, respectively.[24] Intra-ocular reliability was poorer, with ICCs of 0.35 ($p = .219$) and 0.37 ($p = .102$) for the EZ/RPE20% and EZ/ONL ratios, respectively (Table 2).

Further analysis of intra-ocular differences in reflectivity with dot-plots showed a greater dispersion of data for the peripheral scan location but gave no indication of a clear direction of effect. Foveal or peripheral location was not associated with a higher or lower relative EZ reflectivity (Wilcoxon signed-rank test: $p = .569$ and $p = .204$ for EZ/RPE20% ratio and EZ/ONL ratio, respectively) (Figure S1)

Associations EZ reflectivity and covariates

Univariable regression analyses were performed to explore associations of covariates with relative EZ reflectivity. This revealed a negative linear association of age with EZ/RPE20% ($\rho = 0.28$, $p = .005$) and EZ/ONL ($\rho = 0.25$, $p = .018$). EZ reflectivity did not significantly differ between males and females (EZ/RPE20%: 0.71 vs. 0.64; $p = .064$ and EZ/ONL: 2.67 vs. 2.36; $p = .090$). Furthermore, there were significant associations with IRL thickness (EZ/RPE20%: $\rho = 0.28$; $p = .018$ and EZ/ONL: $\rho = 0.29$; $p = .018$), GCIPL thickness (EZ/RPE20%: $\rho = 0.33$; $p = .003$ and EZ/ONL: $\rho = 0.36$; $p = 0.005$)) and EZ thickness (EZ/RPE20%: $\rho = 0.23$; $p = .029$ and EZ/ONL: $\rho = 0.16$; $p = .102$). There were significant associations between reflectivity and OCT scan quality (measured in signal-to-noise ratio in dB) for both the EZ/RPE20% ratio ($\rho = 0.43$; $p < .001$) and the EZ/ONL ratio ($\rho = 0.51$; $p < 0.001$) (Figure S2).

A likely explanation is that scan quality is generally lower in disease, due, for example, to lower visual acuity.

EZ reflectivity in CPEO, DOA, and PPON

The Kruskal–Wallis test indicated there was strong evidence for differences between the control group, CPEO patients, DOA patients, and PPON patients for both the EZ/RPE20% and the EZ/ONL ratios ($p = .003$ and $p = 0.004$, respectively). Post-hoc analysis revealed that there was a significant difference between the control group and the CPEO group ($p = 0.034$ and $p = .011$) and the PPON group ($p = .002$ and $p = .007$) for both the EZ/RPE20% and the EZ/ONL ratios, respectively (Table 3 and Figure 2). For the DOA group, there was only a significant difference for the EZ/RPE20% ratio ($p = .048$).

Multivariable linear regression models were built to account for the potential confounding effects of covariates (Table 4 and Figure 2). CPEO, DOA, and PPON were associated with significantly lower EZ reflectivity, both when normalised to the RPE20% layer and the ONL layer, when adjusted for age, sex, and IRL thickness. In the subsequent model, adjusted for age, sex, and GCIPL thickness, CPEO was associated with

Table 3. EZ/RPE20% ratio and EZ/ONL ratio across the groups. CPEO = chronic progressive external ophthalmoplegia. DOA = dominant optic atrophy. PPON= primary progressive optic neuropathy.

	EZ/RPE20% median (range)	EZ/ONL median (range)
Controls	0.75 (0.64–0.91)	2.95 (1.94–3.45)
CPEO	0.62 (0.57–0.74)	2.29 (2.06–2.63)
DOA	0.68 (0.52–0.79)	2.54 (1.69–3.18)
PPON	0.60 (0.44–0.77)	2.37 (2.03–2.72)
p-value	0.003	0.003

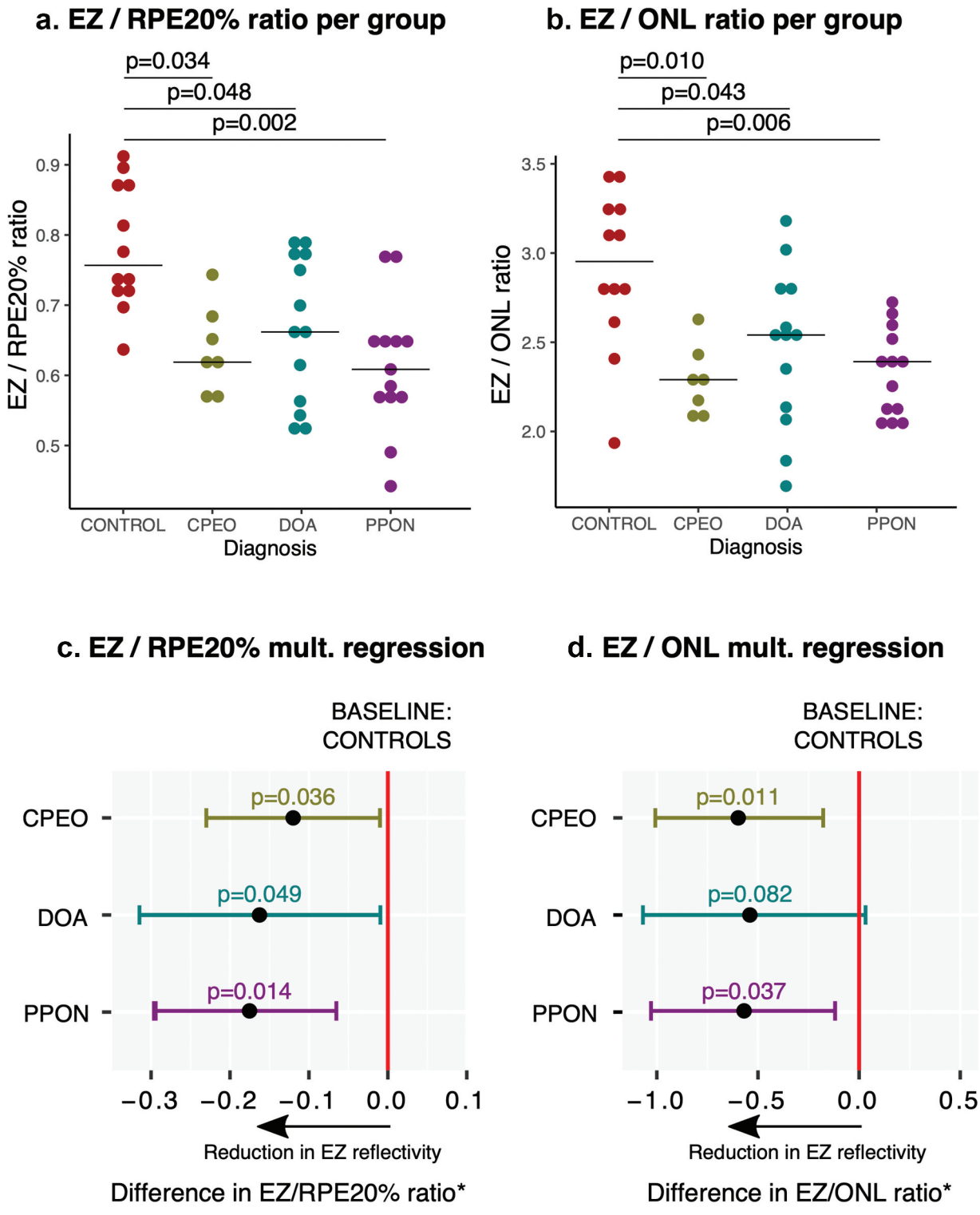

Figure 2. Relative EZ reflectivity in controls and patients with CPEO, DOA, and PPON. Panels a and B display the distributions of the RZ/RPE20% ratio and the EZ/ONL ratio, respectively across these groups. The *p*-values indicate post-hoc analysis results using the Dunn-test (adjusted for multiples comparisons). Panels C and D illustrate the outcomes of multivariable regression analysis, adjusted for sex, age, and inner retinal layer thickness. The bars represent 95% confidence intervals.

Table 4. Results of multivariable linear regression analysis investigating the associations of EZ/RPE20% and EZ/ONL with disease status (controls, CPEO, DOA and PPON) with adjustments made for sex, age, inner retinal layer thickness (model 1), ganglion cell, and inner plexiform layer thickness (model 2), or ellipsoid zone layer thickness (model 3), and further adjusted for signal-to-noise ratio (model 4). No independent significant associations were observed for sex, age, or retinal layer thickness; however, a near-significant association with signal-to-noise ratio is demonstrated.

		EZ/RPE20% ratio			EZ/ONL ratio		
		Estimate	*p*-value	95% CI	Estimate	*p*-value	95% CI
	Multivariable linear regression adjusted for age, sex and IRL thickness						
Diagnosis (BL = control)	**CPEO**	−0.12	**.036**	−0.22 – −0.02	−0.59	**.011**	−0.98 – −0.20
	DOA	−0.16	**.049**	−0.31 – −0.01	−0.55	.082	−1.15–0.10
	PPON	−0.17	**.014**	−0.28 – −0.06	−0.57	**.037**	−1.08 – −0.06
	Multivariable linear regression adjusted for age, sex and GCIPL thickness						
Diagnosis (BL = control)	**CPEO**	−0.09	.096	−0.20–0.02	−0.52	**.022**	−0.98 – −0.06
	DOA	−0.05	.577	−0.19–0.11	−0.28	.443	−0.66–0.10
	PPON	−0.08	.286	−0.22–0.06	−0.35	.270	−0.75–0.05
	Multivariable linear regression adjusted for age, sex and EZ thickness						
Diagnosis (BL = control)	**CPEO**	−0.10	.063	−0.21–0.01	−0.51	**.015**	−0.97 – −0.04
	DOA	−0.12	**.003**	−0.20 – −0.04	−0.45	**.004**	−0.85 – −0.05
	PPON	−0.13	**.002**	−0.20 – −0.05	−0.45	**.006**	−0.86 – −0.04
	Multivariable linear regression adjusted for signal-to-noise ratio						
Diagnosis (BL = control)	**CPEO**	−0.09	.071	−0.19–0.01	−0.42	**.034**	−0.82 – −0.02
	DOA	−0.06	.147	−0.14–0.02	−0.25	.148	−0.54–0.05
	PPON	−0.12	**.009**	−0.21 – −0.03	−0.38	**.026**	−0.74 – −0.02
Signal-to-noise ratio (dB)		0.01	.075	−0.01–0.01	−0.02	**.042**	−0.03 – −0.01

a significantly lower EZ/ONL ratio ($p = .022$) but not EZ/RPE20% ratio. The final model, adjusted for signal-to-noise ratio, revealed significant and independent reductions in the EZ/RPE20% for PPON and the EZ/ONL ratio for PPON and CPEO. When combining the retinal thickness and scan quality covariates in one model, there were no significant associations of EZ reflectivity with pathology.

EZ reflectivity in acute optic neuritis

Median EZ/RPE20% and the EZ/ONL ratios were lower in the affected eyes (0.70; range: 0.49–0.90 and 2.58; range: 1.90–2.97) and the fellow eyes (0.70; range: 0.41–0.94 and 2.67; range: 1.92–3.06) of acute ON patients compared with controls (0.75; range: 0.64–0.91 and 2.95; range: 1.94–3.45). Affected eyes of ON patients had significantly lower EZ/RPE20% ($p = .045$) and EZ/ONL ratios ($p = .007$) compared with control eyes. Similarly, there was a near-significant reduction in EZ/RPE20% ($p = .076$) and a significant reduction in EZ/ONL ($p = .013$) in fellow eyes of ON patients compared with healthy controls. Wilcoxon signed-rank tests found no evidence for interocular differences in EZ reflectivity between the affected and fellow eyes of ON patients (EZ/RPE20%: $p = .520$ and EZ/ONL: $p = .345$).

Subsequently, the associations of EZ reflectivity with ON status were adjusted for potential confounders using multivariable linear regression (Table 5). This analysis identified a significant reduction of −0.11 in EZ/RPE20% ($p = .013$) and of −0.42 in EZ/ONL ($p = .006$) in affected eyes of acute ON patients compared with controls, when adjusted for scan quality, age, sex, and mGCIPL thickness. There was no significant difference in EZ reflectivity between controls and fellow eyes of acute ON patients.

Discussion

In this study, we introduced an innovative automated analysis tool capable of extracting EZ reflectivity from macular OCT scans with excellent test–retest reliability. Moreover, our preliminary findings suggest that relative EZ reflectivity may be reduced in both neuroinflammatory diseases and disorders associated with mitochondrial failure. While this holds exciting potential for monitoring cellular function in vivo, further research is essential to establish EZ reflectivity as a non-invasive biomarker of mitochondrial function.

The evaluation of test–retest reliability was enabled by the availability of repeated OCT scans, revealing strong performance for the EZ/RPE20% ratio, and moderate-to-good reliability for the EZ/

Table 5. Results of multivariable linear regression analysis investigating the associations of EZ/RPE20% and EZ/ONL with optic neuritis status. The analysis is adjusted for scan quality, age, sex, and GCIPL thickness. Healthy controls are compared with the affected eyes (model 1) and the fellow eyes (model 2) of on patients.

		EZ/RPE20% ratio			EZ/ONL ratio		
		Estimate	*p*-value	95% CI	Estimate	*p*-value	95% CI
	Multivariable linear regression adjusted for age, sex, GCIPL thickness and scan quality						
Diagnosis (BL=control)	**Acute ON (affected eye)**	−0.11	**.013**	−0.19 – −0.03	−0.42	**.006**	−0.72 – −0.10
Scan quality (dB)		0.00	.335	0.00–0.00	0.02	**.027**	0.01–0.03
Age (per year)		−0.00	**.029**	−0.01–0.00	−0.01	.182	−0.02–0.01
Sex	**Male**	0.00	.929	0.00–0.00	−0.09	.519	−0.29–0.11
GCIPL (per micron)		−0.00	.081	−0.00–0.00	−0.01	.209	−0.02–0.01
	Multivariable linear regression adjusted for age, sex, GCIPL thickness and scan quality						
Diagnosis (BL=control)	**Acute ON (fellow eye)**	−0.09	.268	−0.22–0.05	−0.35	.316	−0.91–0.21
Scan quality (dB)		0.00	.535	0.00–0.00	0.03	.292	−0.02–0.08
Age (per year)		−0.00	.872	−0.00–0.00	−0.00	.870	−0.00–0.00
Sex	**Male**	−0.05	.436	−0.17–0.07	−0.21	.469	−0.62–0.20
GCIPL (per micron)		−0.00	.400	0.00–0.00	−0.01	.457	−0.02–0.01

ONL ratio. Comparable test–retest data and interocular comparisons were observed for the presented EZ reflectivity analysis tool and other methods aimed at extracting layer reflectivity data from OCT scans.[25,26]

Additional methods were employed to further investigate the validity of our methodology, we normalised EZ reflectivity to the RPE and to the ONL layers. Our findings, consistently observed in the EZ/RPE20% and EZ/ONL ratios, support the notion that the identified associations are attributed to changes in the EZ rather than in the reference layers. Furthermore, these results align with previous studies demonstrating reduced EZ reflectivity in other optic nerve and retinal disorders, including glaucoma, AMD, retinitis pigmentosa, and Best disease.[11,14,16,27,28]

The reductions in EZ reflectivity reported here may be linked to changes in mitochondrial health or metabolic function. The high reflectivity of the EZ is believed to arise from light scattering by local accumulations of mitochondria.[2] Therefore, changes in mitochondrial morphology and function may potentially influence EZ reflectivity.[8,29] Other research suggests that EZ reflectivity may represent a broader measure of photoreceptor health, as it correlates with cone density and electrophysiological retinal function.[30] The association between EZ reflectivity and mitochondrial function remains a topic of controversy, EZ reflectivity perhaps being a more general measure of photoreceptor health. However, regardless of anatomical origin there appear to be interesting associations with pathology, to which the present study has contributed.

The choice of reference layer and the methodology are the greatest challenges. There are advantages as well as disadvantages to each retinal layer. In this study we chose the RPE, because of its similar intensity to the EZ, and the ONL, because of its large size and spatial proximity to the EZ. These data suggest that the EZ/RPE20% ratio is superior for quantifying EZ reflectivity, compared with the EZ/ONL ratio. The EZ/RPE20% ratio has higher test reliability, shows less variability within groups and has more robust results in our analysis. This might be because the ONL has high directional reflectivity, with the Henle Fiber Layer increasing reflectivity with off-axis beam placement. The Stiles Crawford effect is the phenomenon that the light scattering ability of cones changes depending on the direction of light entering the pupil, it affects the quantity of reflected light in an unpredictable way. The effect is not only due to the orientation of the cones but also influenced by changes in the distribution of cones and rods moving more peripherally from the fovea. This may have influenced results. However, all analysed scans were focused on the fovea and passed OSCAR-IB quality control criteria, showing no visual signs of off-axis beam placement. Completely controlling for the Stiles Crawford effect is technically complex and remains an important focus for future research within this field.

Although there is only very limited evidence that structural changes occur in the ONL in ON or DOA, there is some evidence that functional changes occur and OPA1 is expressed in the ONL.[31,32] Disease processes affecting the ONL

could theoretically have confounded the findings reported here. The external limiting membrane (ELM) holds great potential as a reference layer within the field of optic neuropathies, given its non-neural origin, this study was not able to explore it given challenges in segmentation of this thin layer. Both segmentation programs used here do not delineate the ELM. In future studies, its potential should be further explored.

This study identified significant reductions in EZ reflectivity in CPEO and DOA. Both diseases are caused by mitochondrial dysfunction, potentially explaining these findings. We also identified reductions in ON and in PPON. Although not proven, an important role for metabolic dysfunction has been postulated in the pathophysiology of acute ON as well as in MS in general.[33] PPON is a rare MS phenotype in which patients have painless progressive optic neuropathy independent of acute inflammatory activity as seen in typical ON.[20] Its pathophysiology likely relates mainly to the neurodegenerative and progressive features of MS, in which metabolic failure is heavily implicated.[34,35]

In summary, while the identified clinical associations between pathology and EZ reflectivity show promise in EZ reflectivity as a biomarker, many uncertainties remain in the development of EZ reflectivity as a reliable biomarker. These include pupil size, beam directionality, slight inter-device differences in OCT protocols, and the choice of best normalisation method.[36] Not all of these were addressed in this study. However, the authors propose that this relatively simple method may produce a useful measure. Further addressing the above mentioned challenges may further increase its sensitivity and reliability.

While our findings offer valuable insights, this study has several limitations. The retrospective analysis of clinical OCT scans for some patients introduced scan quality discrepancies, and variations in age and sex distributions necessitated multivariable regression adjustments. EZ reflectivity was associated with scan quality. This may have confounded results as scan quality was lower in disease, likely due to lower visual acuity in these groups. There is a small risk of measurement bias due to the few manual corrections that were performed on automated layer segmentations. The potential interrelationship between EZ reflectivity and retinal atrophy, as well as residual confounding from comorbidities, should also be considered when interpreting the results.

To further validate our findings, larger prospective cohort studies with uniform scanning protocols are warranted. Exploring differences in EZ reflectivity among different types of MS and associations with clinical disability scores and serum measures of mitochondrial function are necessary to further investigate its potential as a biomarker.

Conclusion

This study presents a novel automated analysis tool for extracting reliable EZ reflectivity from macular OCT scans. Preliminary data indicate reduced EZ reflectivity in neuroinflammatory diseases and mitochondrial disorders. However, the interpretation of results is complex due to limitations in design and sample size. Therefore, larger prospective cohort studies are needed to ascertain the potential of EZ reflectivity as a non-invasive in-vivo biomarker of mitochondrial health, opening new avenues for understanding cellular function in a wide range of disease conditions, both primarily ophthalmic and more generally.

Acknowledgments

We thank the ECTRIMS for funding IK through the post-doctoral international research grant.

Author contributions

Conceptualization, IK, AP. methodology, IK, AP, GTP, AT.; software, DVV.; formal analysis, IK, AP; data curation, IK, AP; visualizatiom, V.D.P., B.T., P.B. and A.M.A.; writing – original draft preparation, IK.; writing – review and editing, IK, DVV, AP, GTP, AT.; supervision, AP, GTP, AT.

Disclosure statement

IK, DVV, AT, and GTP report no conflicts of interest. AP received grant support for remyelination trials in multiple sclerosis to the Amsterdam University Medical Centre, Department of Neurology, MS Centre (RESTORE trial), and UCL, London RECOVER trial; received grant fees from Fight

for Sight (nimodipine in optic neuritis trial); received royalties or licenses from Up-to-Date (Wolters Kluwer) for a book chapter; received speaker fees for the Heidelberg Academy; participates on advisory board for SC Zeiss OCTA Angi-Network, and the SC Novartis OCTiMS study; holds leadership roles for governing board IMSVISUAL; was chairman of ERN-EYE Neuro-ophthalmology (until Oct, 2020); is board member of National Dutch Neuro-ophthalmology Association; received equipment from OCTA from Zeiss (Plex Elite); and received medical writing support from Novartis for a manuscript (https://doi.org/10.1002/acn3.51473).

Funding

IK: received postdoctoral research exchange fellowship from ECTRIMS.

References

1. Kleerekooper I, Petzold A, Trip SA. Anterior visual system imaging to investigate energy failure in multiple sclerosis. *Brain*. 2020;143(7):1999–2008. doi:10.1093/brain/awaa049.
2. Cuenca N, Ortuño-Lizarán I, Pinilla I. Cellular characterization of OCT and outer retinal bands using specific immunohistochemistry markers and clinical implications. *Ophthalmology*. 2018;125:407–422. doi:10.1016/j.ophtha.2017.09.016.
3. Litts KM, Zhang Y, Freund KB, Curcio CA. Optical coherence tomography and histology of age-related macular degeneration support mitochondria as reflectivity sources. *Retina*. 2018;38(3):445–461. doi:10.1097/IAE.0000000000001946.
4. Ball JM, Chen S, Li W. Mitochondria in cone photoreceptors act as microlenses to enhance photon delivery and confer directional sensitivity to light. *Sci Adv*. 2022;8:1–13. doi:10.1126/sciadv.abn2070.
5. Curcio CA, Sloan KR, Kalina RE, Hendrickson AE. Human photoreceptor topography. *J Comp Neurol*. 1990;292(4):497–523. doi:10.1002/cne.902920402.
6. Wilson JD, Cottrell WJ, Foster TH. Index-of-refraction-dependent subcellular light scattering observed with organelle-specific dyes. *J Biomed Opt*. 2007;12:014010. doi:10.1117/1.2437765.
7. Beauvoit B, Evans S, Jenkins T, Miller EE, Chance B. Correlation between the light scattering and mitochondrial content of normal tissues and transplantable rodent tumors. *Anal Biochem*. 1995;226:167–174. doi:10.1006/abio.1995.1205.
8. Tychinsky V. The metabolic component of cellular refractivity and its importance for optical cytometry. *J Biophotonics*. 2009;2:494–504. doi:10.1002/jbio.200910042.
9. Pasternack RM, Zheng J-Y, Boustany NN. Optical scatter changes at the onset of apoptosis are spatially associated with mitochondria. *J Biomed Opt*. 2010;15:040504. doi:10.1117/1.3467501.
10. Pasternack RM, Zheng JY, Boustany NN. Detection of mitochondrial fission with orientation-dependent optical Fourier filters. *Cytom Part A*. 2011;79A:137–148. doi:10.1002/cyto.a.21011.
11. Tao LW, Wu Z, Guymer RH, Luu CD. Ellipsoid zone on optical coherence tomography: a review. *Clin Exp Ophthalmol*. 2016;44(5):422–430. doi:10.1111/ceo.12685.
12. Akyol E, Hagag AM, Sivaprasad S, Lotery AJ. Adaptive optics: principles and applications in ophthalmology. *Eye*. 2021;35:244–264. doi:10.1038/s41433-020-01286-z.
13. Wu Z, Ayton LN, Guymer RH, Luu CD. Relationship between the second reflective band on optical coherence tomography and multifocal electroretinography in age-related macular degeneration. *Investig Ophthalmol Vis Sci*. 2013;54(4):2800–2806. doi:10.1167/iovs.13-11613.
14. Thiele S, Isselmann B, Pfau M, et al. Validation of an automated quantification of relative ellipsoid zone reflectivity on spectral domain-optical coherence tomography images. *Transl Vis Sci Technol*. 2020;9(11):1–10. doi:10.1167/tvst.9.11.17.
15. Toprak I, Yaylalı V, Yildirim C. Early deterioration in ellipsoid zone in eyes with non-neovascular age-related macular degeneration. *Int Ophthalmol*. 2017;37:801–806. doi:10.1007/s10792-016-0331-3.
16. Ha A, Kim YK, Jeoung JW, Park KH. Ellipsoid zone change according to glaucoma stage advancement. *Am J Ophthalmol*. 2018;192:1–9. doi:10.1016/j.ajo.2018.04.025.
17. Thiele S, Wu Z, Isselmann B, Pfau M, Guymer RH, Luu CD. Natural history of the relative ellipsoid zone reflectivity in age-related macular degeneration. *Ophthalmology Retina*. 2022;6:1165–1172. doi:10.1016/j.oret.2022.06.001.
18. Desai RA, Smith KJ. Experimental autoimmune encephalomyelitis from a tissue energy perspective. *F1000Research*. 2017;6:1973. doi:10.12688/f1000research.11839.1.
19. Campbell GR, Worrall JT, Mahad DJ. The central role of mitochondria in axonal degeneration in multiple sclerosis. *Mult Scler J*. 2014;20(14):1806–1813. doi:10.1177/1352458514544537.
20. Petzold A, Fraser CL, Abegg M, et al. Diagnosis and classification of optic neuritis. *Lancet Neurol*. 2022;21(12):1120–1134. doi:10.1016/S1474-4422(22)00200-9.
21. Tewarie P, Balk L, Costello F, Villoslada P, et al. The OSCAR-IB consensus criteria for retinal OCT quality assessment. *PLOS ONE*. 2012;7(4):1–7. doi:10.1371/journal.pone.0034823.
22. Aytulun A, Cruz-Herranz A, Aktas O, et al. The APOSTEL 2.0 recommendations for reporting quantitative optical coherence tomography studies. 2021.

23. Koo TK, Li MY. A guideline of selecting and reporting intraclass correlation coefficients for reliability research. *J Chiropr Med*. 2016;15:155–163. doi:10.1016/j.jcm.2016.02.012.
24. Cicchetti DV. Interreliability standards in psychological evaluations. *Psychol Assess*. 1994;6:284–290. doi:10.1037/1040-3590.6.4.284.
25. Risseeuw S, Bennink E, Poirot MG, et al. A reflectivity measure to quantify bruch's membrane calcification in patients with pseudoxanthoma elasticum using optical coherence tomography. *Transl Vis Sci Technol*. 2020;9(8):1–12. doi:10.1167/tvst.9.8.34.
26. Saßmannshausen M, Behning C, Isselmann B, et al. Relative ellipsoid zone reflectivity and its association with disease severity in age-related macular degeneration: a MACUSTAR study report. *Sci Rep*. 2022;12(1):1–12. doi:10.1038/s41598-022-18875-5.
27. Gong Y, Chen LJ, Pang CP, Chen H. Ellipsoid zone optical intensity reduction as an early biomarker for retinitis pigmentosa. *Acta Ophthalmol*. 2021;99:e215–e221. doi:10.1111/aos.14542.
28. Romano F, Arrigo A, Leone PP, et al. Altered ellipsoid zone reflectivity and deep capillary plexus rarefaction correlate with progression in best disease. *Br J Ophthalmol*. 2020;104(4):461–465. doi:10.1136/bjophthalmol-2019-313980.
29. Wilson JD, Bigelow CE, Calkins DJ, Foster TH. Light scattering from intact cells reports oxidative-stress-induced mitochondrial swelling. *Biophys J*. 2005;88:2929–2938. doi:10.1529/biophysj.104.054528.
30. Saleh M, Flores M, Gauthier AS, et al. Quantitative analysis of photoreceptor layer reflectivity on en-face optical coherence tomography as an estimator of cone density. *Graefe's Arch Clin Exp Ophthalmol*. 2017;255(11):2119–2126. doi:10.1007/s00417-017-3761-3.
31. Al-Louzi OA, Bhargava P, Newsome SD, et al. Outer retinal changes following acute optic neuritis. *Mult Scler J*. 2016;22(3):362–372. doi:10.1177/1352458515590646.
32. Schild AM, Ristau T, Fricke J, et al. SDOCT thickness measurements of various retinal layers in patients with autosomal dominant optic atrophy due to OPA1 mutations. *Biomed Res Int*. 2013;2013. doi:10.1155/2013/121398.
33. Thompson AJ, Baranzini SE, Geurts J, et al. Multiple sclerosis. *Lancet*. 2018;391(10130):1622–1636. doi:10.1016/S0140-6736(18)30481-1.
34. Mahad DH, Trapp BD, Lassmann H. Pathological mechanisms in progressive multiple sclerosis. *Lancet Neurol*. 2015;14:183–193. doi:10.1016/S1474-4422(14)70256-X.
35. Witte ME, Mahad DJ, Lassmann H, van Horssen J. Mitochondrial dysfunction contributes to neurodegeneration in multiple sclerosis. *Trends Mol Med*. 2014;20:179–187. doi:10.1016/j.molmed.2013.11.007.
36. Lee KE, Heitkotter H, Carroll J. Challenges associated with ellipsoid zone intensity measurements using optical coherence tomography. *Transl Vis Sci Technol*. 2021;10(12):1–14. doi:10.1167/tvst.10.12.27.